Development of Turbulent Mixing at a Gas-Liquid Interface at Accelerations from 10^2 g_0 to 10^5 g_0 and Pressures from 1 to 400 atm

N.V.Nevmerzhitsky, M.V.Bliznetsov, V.A.Girin, V.I.Kozlov, A.K.Lychagin, A.N.Razin, E.A.Sotskov, V.A.Ustinenko

Russian Federal Nuclear Center – VNIIEF, Sarov

Report on
9th International Workshop on the Physics of Compressible Turbulent Mixing
(Cambridge, UK, July 2004)

ABSTRACT

Experimental and numerical results on development of turbulent mixing caused by Rayleigh-Taylor instability at the surface of a liquid layer accelerated by compressed gas. Water was used as liquid and compressed helium (He) as gas. Acceleration of the liquid layer was varied from $\approx 10^2 g_0$ to $\approx 10^5 g_0$ (g_0=9.81 m/s^2) by compressing the accelerating gas from pressure of ≈1 atm to ≈400 atm, which increased its temperature from ≈293°K to 2000°K. The water layer was displaced by about 20 mm.

Preliminary analysis of experimental data showed that the speed of gas front penetration into liquid decreases considerably as the acceleration of the liquid layer increases (this increases gas pressure and temperature). The authors believe this phenomenon can be accounted for by change of turbulent mixing zone structure as a result of decreasing surface tension and the role of viscosity in turbulent mixing development in the experiments.

INTRODUCTION

It is essential for all trends of inertial confined fusion (ICF) that fluids stay pure and unmixed at fusion target interfaces. Turbulent mixing (TM) between fluids caused by Rayleigh-Taylor (R-T) and Richtmyer-Meshkov (R-M) instabilities[1; 2; 3] at interfaces decreases working gas compression and temperature and, therefore, neutron yield in ICF [4]. So, TM effects on system dynamics in such devices must be handled correctly. Both numerical methods and various types of semi-empirical models are used to treat TM in ICF. Both must be benchmarked against data obtained in model experimental studies.

It is believed that at constant acceleration TM zone width develops according to the following law: $L = \alpha(1+k)Agt^2$, where A is Atwood number, k is mixing asymmetry degree, g is acceleration, t is time. Published experimental data and direct numerical simulation results provide different estimates for the parameter α [5, 6], which suggests that further research is needed to determine this law more accurately and to identify factors that influence TM zone growth. Surface tension and viscosity are known (e.g., [7]) to play a stabilizing role at the beginning of R-T instability (when initial perturbations are growing). The role of these factors at TM stage is not yet completely understood. Perhaps, their effects will be most clearly pronounced at higher accelerations. At present there are no experimental studies at accelerations $g > 10^3 g_0$. It is quite difficult to understand the role of surface tension, Reynolds number, compressibility on TM development from published experimental data measured at low g ($g \le 10^3 g_0$).

This paper presents a technique and results of an experimental study on TM zone development in case of Rayleigh-Taylor instability at a gas-liquid interface at accelerations within $10^2 g_0 \le g \le 10^5 g_0$ ($P \approx 1 \div 400$ atm, $T \approx 293°K \div 2000°K$). 1D simulation results and data of two simplified theoretical models are used to understand the system dynamics in tests and to evaluate TM zone width. The authors do not claim that these are complete results: they should be treated rather as a first step in TM investigations at high accelerations. In future, it is planned to continue the experimental work for more detailed investigation of turbulence characteristics and improvement of the numerical model.

THE EXPERIMENTAL TECHNIQUE

A schematic of the test facility is given in figure 1. The device consists of a three-section acceleration channel, CGM (Combustible Gas Mixture) chamber, lid, rigid piston and substrate. The channel inner diameter is 50 mm. Electric spark dischargers for CGM initiation are located at the inner side of the lid. The piston is made of transparent organic glass or polyethylene, the substrate is made of organic glass or textolite. The substrate and the piston were tightened in the channel by special rings. The substrate was tightly clamped between parts of the acceleration channel by a collar and spacers. The lower edge of the channel was open: connected to the atmospheric space.

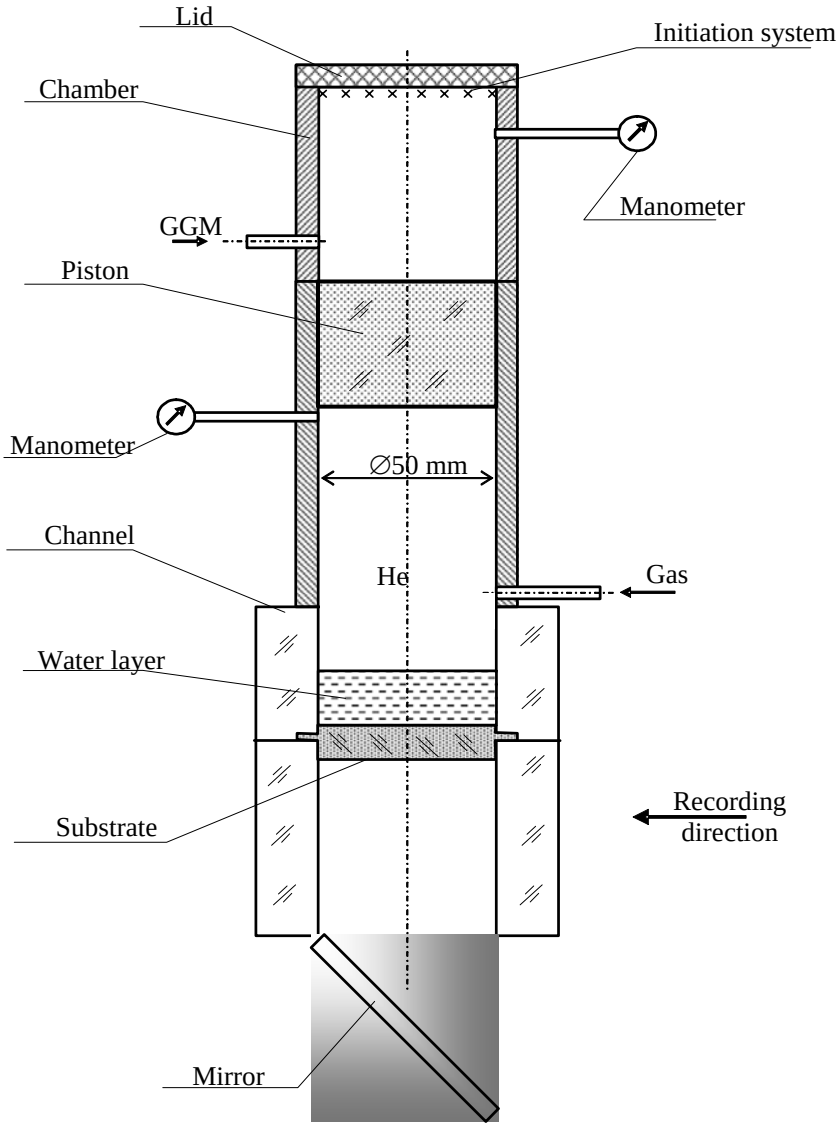

Figure 1 – Schematic of experimental facility.

Water was used as the heavy layer in the tests. Water was poured in the acceleration channel on the substrate or in a transparent container. The total weight of water and the substrate was ≈ 100 g. Initial («start-up») perturbation on water surface were ensured in a number of tests by solid particles with a characteristic size of ≈ 0.4 mm and density 0.91 g/cm^3. They occupied ≈0.5% of the surface area. The channel space between water and the rigid piston was filled with helium, and the CGM chamber was filled with stoichiometric mixture of acetylene and oxygen to a specified pressure.

The layer was accelerated in the following way. After initiation of CGM the piston was accelerated and compressed He below it. When He pressure exceeded the critical value the substrate collar was cut off, and water, together with the substrate, was accelerated vertically downwards. The gas-liquid interface became unstable: TMZ developed on it after some time. Water acceleration was higher in experiments with large initial volume and pressure of CGM, while at lower CGM initial

volume and pressure the acceleration was also lower. In test with $g \approx 10^5 g_0$: the Atwood number A ≈ 0.97, interface density ratio changed during the acceleration time from 200 to 60, the maximum compression of He was about 20 (test #8 at t ≈1.87 ms), temperature in compressed He reached 2000°K.

The tests were recorded by high-speed camera in one or two perpendicular projections: front (lateral) and horizontal (toward the moving layer).

EXPERIMENTAL RESULTS

Figure 2 presents moving image frames from several tests, figure 3 shows processed data of tests with $g \approx 10^2 g_0$ and $g \approx 10^5 g_0$:

- Characteristic curves for liquid layer acceleration as a function of its path g = $g(2S)$. The acceleration was obtained by differentiation of a 4th-order polynomial that approximates experimental $S(t)$;
- Gas front depth in the liquid h_{LT} as a function of S: $\sqrt{h_{LT}}(Y)$, where $Y = \int \sqrt{g}\,dt$. Curve sections within the interval 1≤Y≤4.5 (almost linear) were approximated by a straight line. Inclination angle tangent with respect to the abscissa axis characterizes the rate of TM front penetration into liquid $\beta_{LT} = \left(\Delta\sqrt{h_{LT}}/\Delta Y\right)^2 / A$, here the Atwood number A ≈ 1 (the curves are given in the integral form because the acceleration was variable). The experimental uncertainties are: path S ~ ±0.25 mm; h_{LT} ~ ±0.5 mm; time ~ 0.5%t.

An analysis of moving images and data presented in figures show that:

➢ The rate of gas front penetration into liquid at the initial phase of TM increased in tests with start-up perturbations compared to test with no perturbation specified (see figure 3, tests #4 and #5 at Y<1.5).

➢ The classical pattern of TM development with R-T instability was observed in tests with $g \le 10^3 g_0$: gas penetrated into liquid in quasi-round bubbles, while liquid penetrates in plumes. Bubbles can be seen on the horizontal projection as light circles.

➢ TMZ develops differently in test with $g \approx 10^5 g_0$: no bubbles and plumes can be seen on the frontal projection. This shows that small-scale fractions appear in TMZ structure and screen the photo image. Shaded round spots can be observed on the horizontal projection of the moving image, they are similar to the bubbles seen in previous tests, but these spot almost do not grow and gradually become darker. These “bubbles” could darken because of TMZ development on their inner surface or because of disintegration.

➢ When the liquid layer acceleration grows from $g \approx 5 \cdot 10^2 g_0$ to $g \approx 10^5 g_0$ (i.e. pressure grows from 1 atm to 400 atm and temperature of compressed He increases to 2000°K), β_{LT} decreases from 0.13 to 0.03. The optically observable total TMZ width does not change significantly (see figure 2), which can be attributed to small-scale dispersion of liquid in gas that can change the asymmetry of the zone.

NUMERICAL RESULTS

Numerical simulations of gas-dynamic motion of the system were conducted in 1D using the VIKHR technique [8]. Figure 4 presents the initial geometry for simulations of test No.8 with high acceleration. Table 1 shows initial densities, specific internal energies of materials and equations of state used in simulations. The numerical grid was uniform, the number of points is given in table 1. Detonation velocity in CGM was set to D = 2.45 km/s, and the caloric value was q = 7.21 kJ/g. Perfect gas EOS with γ = 1.16 was used for CGM.

The left boundary that corresponds to the top of the test facility was assumed to be a rigid wall. The right boundary was assumed free: pressure was set equal to the atmospheric pressure. Heat conduction was neglected in the calculations.

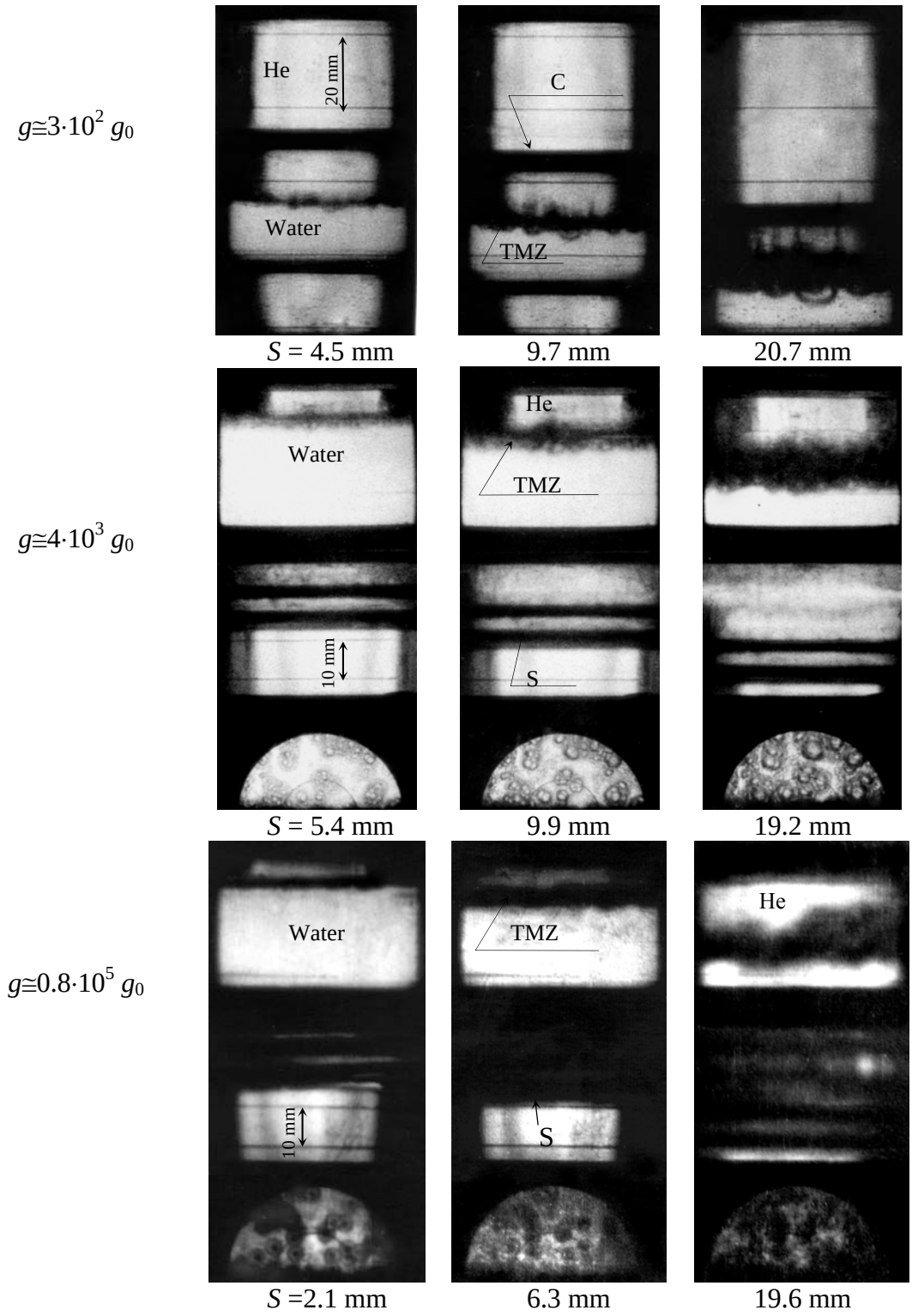

Figure 2 – Moving image frames. Notation: He – compressed helium; TMZ – turbulent mixing zone; C – container; S – substrate.

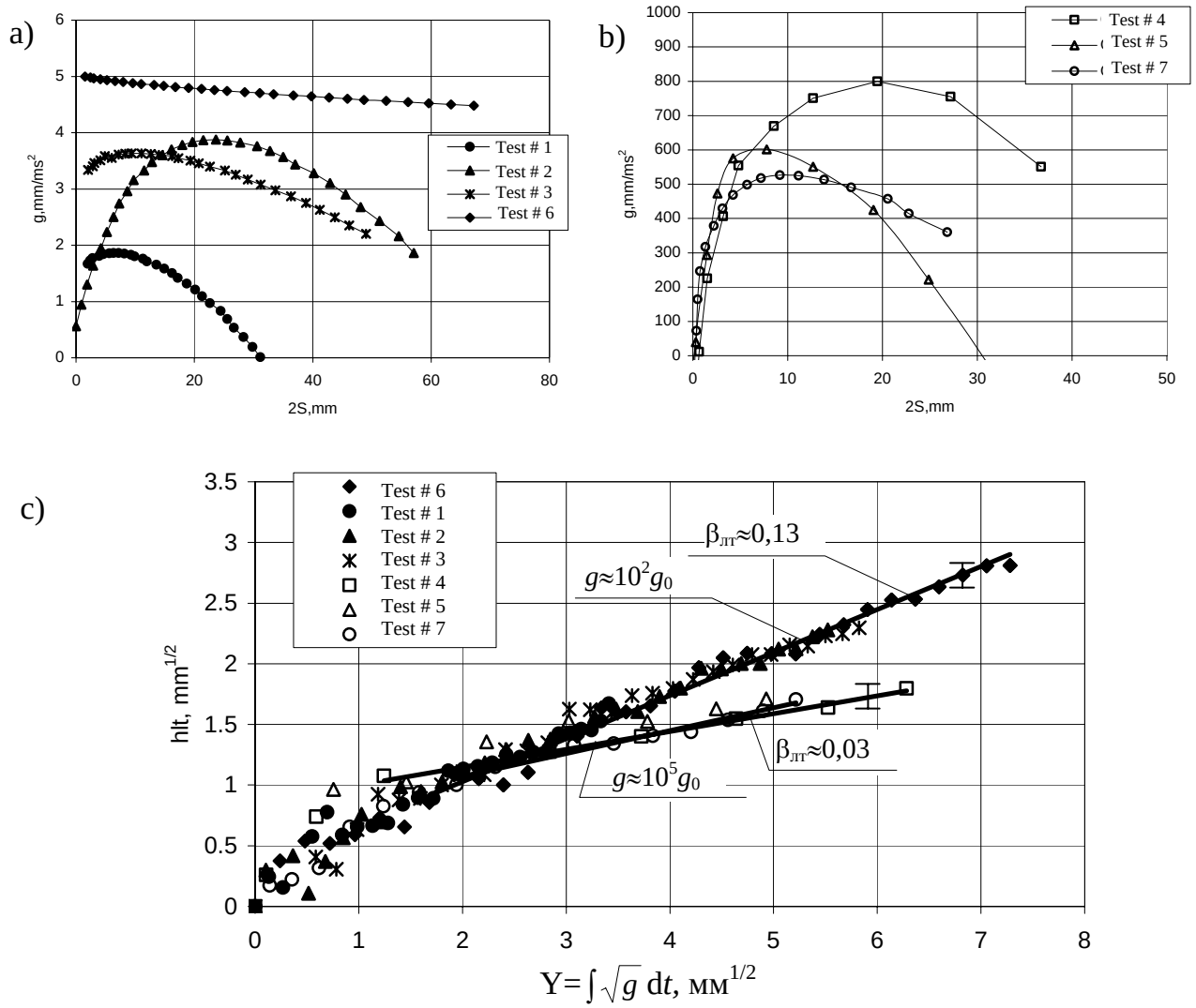

Figure 3 – Processed experimental data on: a), b) layer acceleration; c) gas front penetration into liquid as a function of layer path $Y=\int\sqrt{g}\,dt$; (characteristic tests)

In the tests, the textolite substrate under the water layer started to move after the 1.5-mm-thick collar was cut off, i.e. after pressure on the substrate surface reached $P_c \approx 100$ atm. To account for this effect in simulations at $P < P_c$ on the water-textolite interface, the right boundary of domain 4 was treated as a rigid wall, domains 5 and 6 being ignored in calculations. Domains 5 and 6 were included in the calculation after pressure at the water-textolite interface reached P_c, the right boundary 6 being treated as a free boundary at atmospheric pressure.

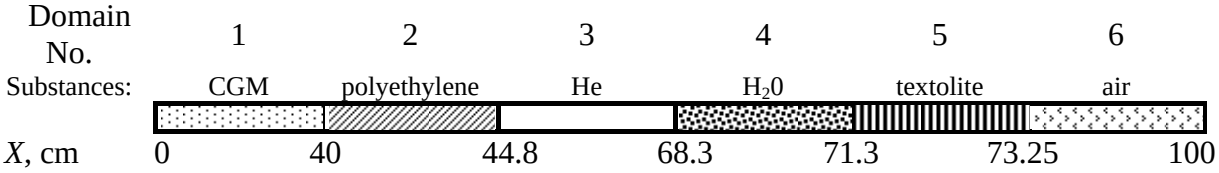

Figure 4 – Initial geometry in the simulation of test # 8

Figure 5 shows *X-t* diagrams of interfaces and shock in test No.8, figure 6 depicts *X-t* diagram of He-water interface after the layer starts to move, figure 7 presents water layer acceleration in simulation without TM. As one can see from figure 6, the calculated X-t diagram of He-water interface is in satisfactory agreement with the experimental measurements.

Table 1 – Input data for the simulation of test No.8

Domain No.	*R*, cm	Substance	EOS	ρ, g/cm^3	*P*, bar	*E*, atm·cm^3/g	Grid
1	40.0	C_2H_2+2.5·O_2	Perfect gas	6.4376E-3	5.2	5.14493E+3	500
2	44.8	CH_2	Mie-Gr.	0.92	4	4.348	25
3	68.3		Perfect gas	6.5713E-4	4	9.08519E+3	400
4	71.3	H_2O	Mie-Gr.	1.000	4	10.000	200
5	73.25	Textolite	Mie-Gr.	1.300	4	3.077	100
6	100	air	Perfect gas	1.3E-3	1	1.92308E+3	600

Let's estimate TMZ growth based on Belenky –Fradkin [9] and Youngs [10, 11] models. Notice that viscosity and surface tension are not taken into account in these models.

Turbulent mixing zone evolution in the Youngs model is described by relationships resulting from the balance between Archimedean and drag forces when bubbles and plumes move:

$$\frac{dU_1}{dt} = Ag - C\frac{U_1|U_1|}{h_1}, \qquad \frac{dU_2}{dt} = Ag - \frac{C}{\sqrt{\delta}}\frac{U_2|U_2|}{h_1}, \qquad U_i = \frac{dh_i}{dt}.$$

Subscript «1» relates to bubbles of the light fluid, and «2» shows plumes of the heavy one, δ is the interface density ratio, A is Atwood number. The parameter C = 3.67 was chosen by Youngs based on best fit to various experimental data. When integrating the above system of equations the initial perturbation was set to 0.2 mm, and the acceleration was in accordance with the solid curve in figure 7.

According to Belenky –Fradkin (B-F) model [9], turbulent mixing zone width is given by:

$$L = \alpha^4 \left(\eta_1 + \eta_2\right)^5 \left(\int_0^t \sqrt{g(z)}\, dz\right)^2,$$

where $\eta_2 = 2.8354$, $\eta_2 = 1.5988$. TMZ degree of asymmetry in this model is k = η_2/η_1 = 1.773 for the interface density ratio $\delta = 100$. The proportionality coefficient between TMZ and mixing length $l_t = \alpha \cdot L$ in the paper by B – F was set to 0.133. The value α = 0.133 was chosen in B – F based on measured TMZ width growth rate at low Atwood numbers. In our case, α = 0.113 was obtained by benchmarking against experimental data on He penetration depth in water.

Figure 8 shows a comparison between calculations with these models and experimental data of test #8. It follows from figure 8 the Youngs model satisfactorily describes TMZ growth and asymmetry when acceleration is working. The B-F model could not describe experimental asymmetry of the mixing zone even after benchmarking against data on He penetration depth in water. The VIKHR technique satisfactorily describes penetration of gas into liquid when the acceleration is growing.

CONCLUSIONS

The experimental results show that when the liquid layer acceleration increases from $g \approx 5 \cdot 10^2 g_0$ to $g \approx 10^5 g_0$, accelerating gas pressure increases from 1 to 400 atm and temperature from ≈300 to ≈2000°K, small-scale structures appear in the turbulent mixing zone, and gas penetration into liquid slows down.

Slower penetration of gas front into the liquid at higher accelerations (i.e. higher Reynolds numbers) can be accounted for by changing character of the mixing: the role of viscosity in TM evolution decreases at high accelerations, while increasing pressure and temperature of the accelerating gas decrease surface tension [12] at the interface. These factors stimulate development of short-wave perturbations, from which small "bubbles" form in TMZ. These small bubbles grow into liquid more slowly than large ones (e.g. [13]). Liquid plumes disintegrate into small fragments due to low surface tension and high acceleration.

At low *g*, *P* and *T* surface tension and viscosity are essential for TM evolution. They suppress development of small-scale structure in the turbulent mixing zone, so large bubbles mainly develop, and they grow into liquid faster than small ones, so gas penetrates into liquid at higher rate.

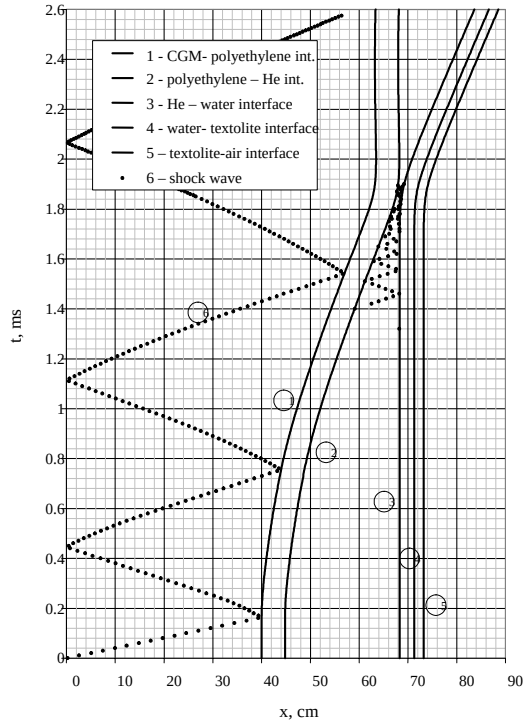

Figure 5 – x-t diagrams of interfaces between domains and shock wave in calculation without TM

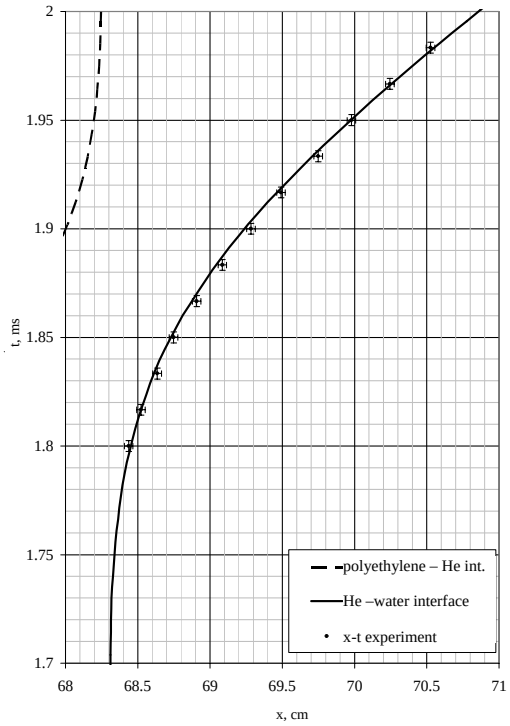

Figure 6 – x-t diagram of He-water interface in experiment and calculation without TM, where $X_{exp} = X_{exp\ water\text{-}textolite} - h_{water}$

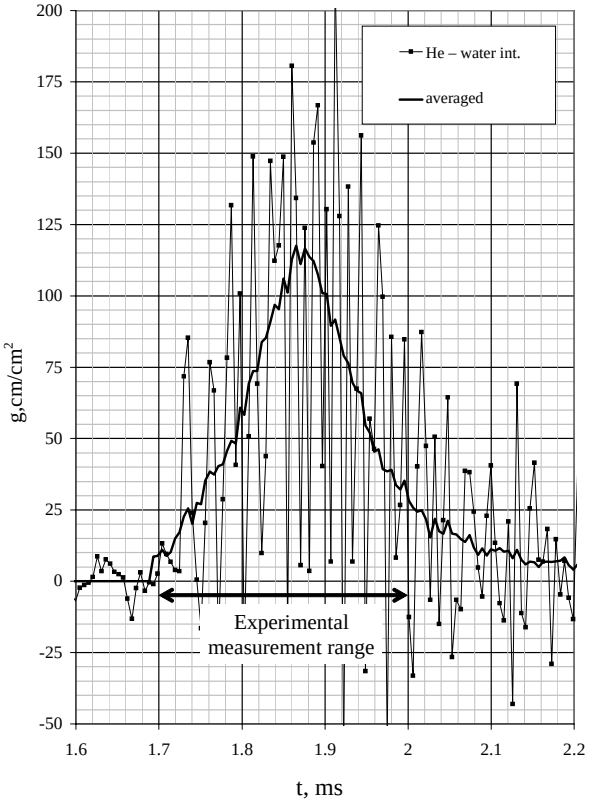

Figure 7 – Water layer acceleration in calculation without TM

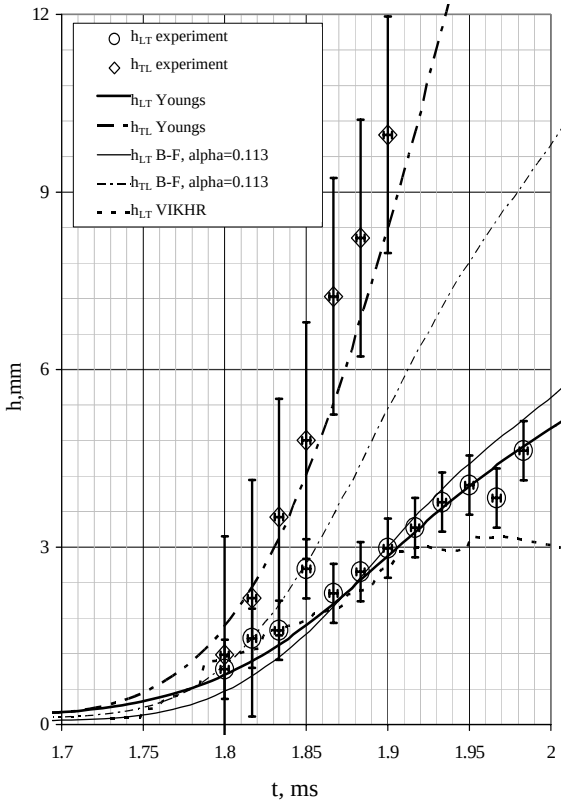

Figure 8 – Comparison of He and water interpenetration depth

The observed TMZ evolution pattern when acceleration is acting at $g \approx 105 \cdot g_0$ is satisfactorily described by D.Youngs model.

In future it is planned to study TMZ structure in more detail and to increase experimental observation time, since TMZ evolution after the end of acceleration pulse is of undoubted interest.

The authors would like to thank: *E.E.Meshkov, V.A.Rayevsky, A.V.Pevnitsky* for very helpful comments and suggestions on this work; *O.L.Krivonos, E.D.Senkovsky,V.I.Dudin,A.A.Nikulin* – for the assistance in performing the experiments.

REFERENCES

1. *Lord Rayleigh.* Proc. London Math. Soc., 1883, v.14, p.170
2. *G.I. Taylor.* The Instability of Liquid Surfaces when Accelerated in a Direction Perpendicular to Their Planes. I. Proc.Roy.Soc., 1950, v.A201, p.192
3. *Meshkov E.E..* Instability at an Interface between Two Gases Accelerated by a Shock Wave. Izvestiya AN SSSR, MZhG, 1969, # 5, p.151-158
4. *Rozanov V.B., Lebo I.G., Zaitsev S.G., Zhidov I.G., Meshkov E.E.., Nevmerzhitsky N.V. et. al.* Experimental Study of Gravitation-Driven Instability and Turbulent Mixing of Stratified Flows in an Acceleration Field Related to Inertial Confined Fusion Problems. Moscow: FIAN. Preprint # 56, 1990, p.63
5. *Statsenko V.P., Yanilkin Yu.V., Rebrov S.V., Sinkova O.G., Stadnik A.L., Selchenkova N.I., Uchaev A.Ya.* Investigation of Turbulence Characteristics in Direct Numerical Simulations of Gravitation-Driven Mixing // Voprosy Atomnoy Nauki I Techniki. Series: Matematicheskoye Modelirovaniye Fizicheskikh Processov. 2002. Issue 2. p. 18-29
6. *Anisimov V.I., Kozlovskhih A.S., Baban S.A.* An Analysis of Experimental Results on Turbulent Mixing at Moderate Reynolds Numbers in the Earth's Gravity Field // VII Zababakhin Scientific Conference. Snezhinsk, 2003
7. *D.H.Sharp.* An Overview of Rayleigh-Taylor Instability. Fronts, Interfaces and Patterns. Proc of the Third Ann. Int. Conf of the Center for Nonlinear Studies. Los Alamos, New Mexico, May 1983, North-Holland Physics publishing 1984, p.3-18
8. *Andronov V.A., Kozlov V.I., Nikiforov V.V., Razin A.N., Yudin Yu.A.* A Technique for Turbulent Mixing Calculation in 1D Flows (the VIKHR Technique) // Voprosy Atomnoy Nauki I Techniki. Series: Matematicheskoye Modelirovaniye Fizicheskikh Processov. 1994, issue 2, p.59
9. *Belenky S.Z., Fradkin E.S.* Turbulent Mixing Theory // Trudy FIAN, vol.XXIX, 1965, p.207-238
10. *D.L. Youngs.* Modeling Turbulent Mixing by Rayleigh – Taylor Instability // Physica, D37, p.270-287, 1989
11. *G. Dimonte.* Spanwise Homogeneous Buoyancy-Drag Model for Rayleigh-Taylor Mixing and Experimental Evaluation // Physics of Plasmas, 2000, v.7, № 6, p.2255-2269
12. *Kirillov P.L., Yuriev Yu.S., Bobkov V.P.* Reference-Book on Thermal Hydraulic Calculations (Nuclear Reactors, Heat Exchangers, Steam Generators). Moscow, Energoatomizdat, 1984, p.296
13. *Sotskov E.A., Nevmerzhitsky N.V., Meshkov E.E., Bliznetsov M.V., Drennov O.A., Senkovsku E.D.* Investigation of Local Perturbation Development and Its Interaction with a Turbulent Mixing Zone at a Gas-Jelly Interface. IFV – RFNC-VNIIEF. Proc. of V.V.Nikiforov Workshop on Turbulen Mixing Physics. Russia, Sarov, November, 2002